

# Observation of protein folding/unfolding dynamics of ubiquitin trapped in agarose gel by single-molecule FRET

Li-Ling Yang · Michael W.-P. Kao ·  
Hsin-Liang Chen · Tsong-Shin Lim ·  
Wunshain Fann · Rita P.-Y. Chen

Received: 15 August 2011 / Revised: 13 October 2011 / Accepted: 24 October 2011 / Published online: 9 November 2011  
© European Biophysical Societies' Association 2011

**Abstract** A ubiquitin mutant with two Cys mutations, m[C]q/S65C, was site-specifically labeled with two dye molecules, Alexa Fluor 488 (donor) and Alexa Fluor 594 (acceptor), due to the different reactivity of these two Cys residues. This doubly dye-labeled ubiquitin has lower structural stability than wild-type ubiquitin. Taking advantage of this decreased stability, conformational heterogeneity of this protein under nondenaturing condition was observed at the single-molecule level using single-paired Förster resonance energy transfer (FRET) by trapping the protein in agarose gel. Three conformational

populations corresponding to folded ( $E_{ET} \approx 0.95$ ), loosely packed ( $E_{ET} \approx 0.72$ ), and unfolded ( $E_{ET} \approx 0.22$ ) structures, and the structural transitions between them were observed. Our results suggest that agarose immobilization is good for observing structural dynamics of proteins under native condition.

**Keywords** FRET · Ubiquitin · Folding · Single molecule · Conformational heterogeneity · Agarose

## Abbreviations

m[C]q/S65C	Ubiquitin mutant with Cys inserted between Met1 and Gln2 and with Ser65 mutated to Cys
AF488-m[C]q/S65C	Mutant protein m[C]q/S65C labeled with Alexa Fluor 488 at the m[C]q site
AF488-m[C]q/S65C- AF594	Mutant protein m[C]q/S65C labeled with Alexa Fluor 488 at the m[C]q site and with Alexa Fluor 594 at the S65C site
AF488-S65C	Mutant protein S65C labeled with Alexa Fluor 488 at the S65C site

Li-Ling Yang and Michael W.-P. Kao made an equal contribution.

Dr. Wunshain Fann, formerly of the Institute of Atomic and Molecular Sciences, Academia Sinica, made a great contribution to this work and would have been a corresponding author, but sadly died on 26 September 2008.

L.-L. Yang · M. W.-P. Kao · H.-L. Chen · R. P.-Y. Chen (✉)  
Institute of Biological Chemistry, Academia Sinica, No. 128,  
Sec. 2, Academia Rd, Nankang, Taipei 115, Taiwan  
e-mail: pyc@gate.sinica.edu.tw

L.-L. Yang · H.-L. Chen · W. Fann  
Institute of Atomic and Molecular Sciences, Academia Sinica,  
Taipei 106, Taiwan

L.-L. Yang  
Taiwan International Graduate Program, Academia Sinica,  
Taipei 115, Taiwan

L.-L. Yang  
Department of Physics, National Taiwan University,  
Taipei 106, Taiwan

T.-S. Lim  
Department of Physics, Tunghai University,  
Taichung 407, Taiwan

## Introduction

The conformational dynamics of proteins is believed to be related to molecular recognition and function. Until the advent of single-molecule detection using Förster resonance energy transfer (FRET) (Benjamin 2005; Ha et al. 1999b;

Kapanidis and Weiss 2002; Weiss 2000), small conformational changes were very difficult to explore. As a spectroscopic ruler, FRET can provide invaluable information on the dynamic motion of proteins and even the protein folding/unfolding process (Lipman et al. 2003; Orte et al. 2008; Ratner et al. 2000). Structural heterogeneity has been explored in (i) vesicle-encapsulated cold-shock protein (Csp) (Rhoades et al. 2004) or adenylate kinase (AK) (Rhoades et al. 2003) under mid-transition conditions, (ii) surface-immobilized RNase H under denaturing conditions (Kuzmenkina et al. 2005, 2006), and (iii) freely diffusible Csp (Schuler et al. 2002), protein L (Merchant et al. 2007), chymotrypsin inhibitor 2 (Deniz et al. 2000), or acyl-coenzyme A (CoA) binding protein (Laurence et al. 2005) at different denaturant concentrations. Although the dynamic behavior of a protein is important for its function, structural fluctuations in a protein in its native condition have been rarely reported. This might be because such fluctuation is not sufficiently pronounced or is too rapid to be recorded by single-molecule methods. Most dynamic studies have therefore focused on (i) partially denatured proteins (Deniz et al. 2000; Laurence et al. 2005), (ii) conformational changes during an enzyme reaction (Ha et al. 1999a; Hanson et al. 2007; Tan et al. 2009) and in receptors, e.g., syntaxin (Margittai et al. 2003), a receptor protein with an open–close conformational switch, and (iii) the conformations of synthetic polyproline peptides of different lengths (Best et al. 2007; Schuler et al. 2005).

Ubiquitin is a small globular protein consisting of 76 amino acids; its ubiquitous nature in all eukaryotes suggests its importance in biological systems. It is highly stable over a wide range of pH and temperature (Lenkinski et al. 1977) and is, therefore, a good target in protein folding research. In single-paired FRET (spFRET) studies of proteins, dye labeling is the first challenge (Jacob et al. 2005; Kim et al. 2008). Recently, we used ubiquitin as a target protein to develop a site-specific FRET dye-labeling strategy on a solid surface (Kao et al. 2008). A six-His-tag was added to the C-terminus of ubiquitin for solid-phase immobilization in the labeling step. Two Cys mutations were designed so as to have different solvent accessibilities and were introduced into ubiquitin as dye-labeling sites by site-directed mutagenesis. One mutation, with a single Cys insertion between the first (Met) and second (Gln) residues, was named m[C]q and the other, with a Ser65 → Cys mutation, was denoted S65C, the double mutant being m[C]q/S65C. The donor dye Alexa Fluor 488 was used to label the more reactive Cys, m[C]q, through a thiol-maleimide linkage, while the acceptor dye Alexa Fluor 594 was used to label the less reactive Cys, S65C, under partially denaturing conditions. Both reactions took place on a solid support. Using this strategy, dye conjugation was site

specific, and the double-labeled ubiquitin mutant protein was denoted AF488-m[C]q/S65C-AF594. Our previous report showed by circular dichroism spectroscopy that the overall architecture of the doubly labeled protein was maintained despite the mutations and dye labeling. However, while the structural stability of m[C]q/S65C is the same as that of wild-type ubiquitin, the stability of AF488-m[C]q/S65C-AF594 is substantially lowered. The respective free energy changes of folding ( $\Delta G^{\text{H}_2\text{O}}$ ) for ubiquitin, unlabeled mutant protein m[C]q/S65C, single-labeled mutant protein AF488-m[C]q/S65C, and double-labeled mutant protein AF488-m[C]q/S65C-AF594, derived from chemical denaturation curves were  $-7.1 \pm 0.6$ ,  $-6.1 \pm 0.8$ ,  $-3.0 \pm 1.2$ , and  $-2.2 \pm 0.6$  kcal/mol, respectively (Kao et al. 2008). The  $\Delta G^{\text{H}_2\text{O}}$  difference ( $\Delta\Delta G^{\text{H}_2\text{O}}$ ) between wild-type ubiquitin ( $-7.1 \pm 0.6$  kcal/mol) and AF488-m[C]q/S65C-AF594 ( $-2.2 \pm 0.6$  kcal/mol) was 4.9 kcal/mol. As the refolding rate of AF488-m[C]q/S65C-AF594 is the same as that of wild-type ubiquitin, Kao et al. (2008) suggested that dye labeling does not affect the energy gap between the unfolded and transition states but destabilizes the native state. The protein stability decrease corresponds to a drop in the folded/unfolded population ratio from 158,000 (wild-type ubiquitin) to 35 (AF488-m[C]q/S65C-AF594). Therefore, conformational heterogeneity should be observable for the less stable AF488-m[C]q/S65C-AF594 in the absence of chemical denaturant. In this study, AF488-m[C]q/S65C-AF594 was trapped in agarose and its conformational heterogeneity was studied using the spFRET technique (Fig. 1).

## Materials and methods

### Protein expression and purification

These have been described in our previous publication (Kao et al. 2008). In brief, the human ubiquitin gene was cloned into the pET-11b vector and mutations introduced by site-directed mutagenesis. A His-tag of six His residues was introduced at the C-terminus of the ubiquitin sequence. A mutant with a single Cys insertion between the first (Met) and second (Gln) residues was named m[C]q, and another with a Ser65 → Cys mutation was named S65C; the double mutant was named m[C]q/S65C. All mutant proteins were expressed in *Escherichia coli* BL21(DE3)star and purified by ammonium sulfate precipitation, chromatography on an affinity column (BD TALON<sup>TM</sup>), and gel filtration (HiLoad 16/60 Superdex 75). The collected fractions were dialyzed against deionized water, lyophilized, and stored at  $-20^{\circ}\text{C}$ .

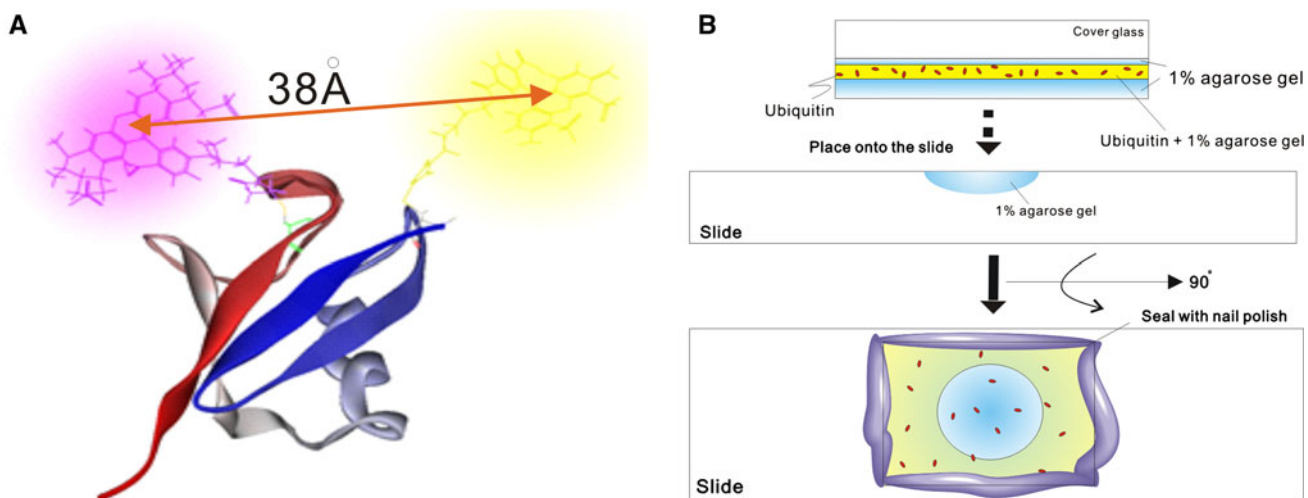


**Fig. 1** Design of the single-molecule FRET experiment. **a** Schematic diagram of the double-labeled ubiquitin molecule AF488-m[C]q/S65C-AF594. Alexa Fluor 488 was labeled onto the m[C]q site of the inserted Cys between Met1 and Gln2. Alexa Fluor 594 was labeled onto the S65C site which corresponds to the Ser65 → Cys mutation. The N-terminal  $\beta$ -hairpin is colored blue, and the  $\beta$ -strand at the

C-terminus red. **b** Illustration of the gel immobilization process. AF488-m[C]q/S65C-AF594 was dissolved in deionized water and mixed with melted agarose. The mixture was spin-coated on an agarose-precoated cover-glass, which was then inverted on top of a concave glass slide filled with the same agarose gel

#### Dye labeling

All steps were carried out at room temperature. Nickel magnetic beads (Millipore) (400  $\mu$ L) were suspended for 5 min in labeling buffer (50 mM sodium phosphate, 300 mM NaCl, 10 mM imidazole, pH 8) in an Eppendorf tube, which was then placed in a magnetic separator, and the liquid removed with a pipette. After 3  $\times$  1 mL washes of the beads with labeling buffer, 1 mg of the protein in 1 mL 2 mM dithiothreitol (DTT) in water was added, and the mixture shaken for 30 min. Nonbound protein was removed as above, then the beads were washed with 3  $\times$  1 mL labeling buffer and 1 mL deionized water. The first dye, Alexa Fluor 488 C5 maleimide (Molecular Probes) (3 equivalents in 1 mL labeling buffer), was then added and reacted for 2 h with shaking. After coupling, excess dye was removed for reuse and the beads washed as above to ensure the dye was completely removed. For the coupling of the second dye, the donor-labeled protein was partially unfolded on the beads by adding 800  $\mu$ L denaturation solution (4 M GdnHCl, 50 mM sodium phosphate, pH 8) and shaking the mixture for 30 min; then, the second dye, Alexa Fluor 594 C5 maleimide (Molecular Probes) (3 equivalents in 200  $\mu$ L of deionized water), was added and reacted for 2 h with shaking. The beads were washed as above and the protein eluted by shaking for 5 min in 200  $\mu$ L elution buffer (50 mM sodium phosphate, 300 mM NaCl, 150 mM imidazole, pH 8). The elution step was repeated a further two times, and the eluted fractions combined and purified by high-performance liquid chromatography (HPLC).

#### Trypsin digestion

Twenty microliters of AF488-m[C]q/S65C (12.5  $\mu$ M) in 50 mM sodium phosphate buffer, pH 7, was incubated for 1 h at 37°C with 5  $\mu$ L trypsin in water (final enzyme concentration 150, 100, 50, 25, 5, or 2.5  $\mu$ M), then the samples were analyzed on a 15% sodium dodecyl sulfate (SDS) polyacrylamide gel. For wild-type ubiquitin, the gel was stained with Coomassie brilliant blue R, while, for AF488-m[C]q/S65C, green fluorescent images were obtained under blue light illumination.

#### Single-molecule experimental setup

Single-molecule experiments were performed on a home-made scanning-stage confocal microscope. A 16-W argon laser (Spectra-Physics Lasers, USA) provided excitation at 488 nm, which was reflected by a dichroic mirror and condensed by an oil-immersion objective (100 $\times$ /1.4 NA oil; Nikon, Japan) to focus on the sample plate. The fluorescence emission was collected by the same objective (Nikon, Japan) and passed through a 500-nm long-pass filter (HQ500LP; Chroma Technology Corp., USA) and two different dichroic mirrors (Omega Optical Inc., USA), the first with a cutoff of 500 nm to further remove excitation light and the second with a cutoff of 550 nm to separate the fluorescence emissions of Alexa Fluor 488 and Alexa Fluor 594, which were detected by two single-photon-counting modules [avalanche photodiodes (APD), SPCM-AQR-15-FC; PerkinElmer Optoelectronics, USA]. Two band-pass filters (HQ535/70 and BP620/60; Chroma

Technology Corp., USA) were introduced in front of the detectors for the donor and acceptor channels to eliminate laser excitation and spectral overlap. For immobilized single-molecule experiments, images were integrated by scanning using a three-axis piezo-scanning stage (P-517.3CL; Physik Instrumente GmbH & Co., Germany) controlled by a commercial scanning controller (E710.4CL; Physik Instrumente GmbH & Co., Germany). Image acquisition was programmed by LabVIEW software (National Instrument, USA). The size of the scanning step was 0.2  $\mu\text{m}$ , and a diffraction spot usually consisted of 3–5 pixels (the point spread function of the confocal system with lateral size of  $\sim 0.2 \mu\text{m}$  and axial size of  $\sim 0.5 \mu\text{m}$  was determined by fluorescence correlation spectroscopy of 10 nM rhodamine 6G).

#### Protein immobilization

To investigate the conformational dynamics, 1% agarose (low melting point; Sigma-Aldrich, USA) in deionized water was melted in a 70°C water bath and cooled to 60°C (ubiquitin is stable over a wide range of pH values and temperatures). AF488-m[C]q/S65C-AF594 was dissolved in deionized water (pH 5) and mixed with the melted agarose at final protein concentration of 500 pM to 5 nM, and the mixture spin-coated on an agarose-precoated cover-glass, which was then inverted on top of a concave glass slide filled with the same agarose gel. As a result, the protein-containing gel layer was sandwiched between two agarose gel films. To maintain humidity, the edges of the cover glass were sealed with nail polish.

#### Anisotropy relaxation measurements

AF488-S65C and pure Alexa Fluor 488 were prepared in deionized water (100 nM, 60  $\mu\text{L}$ ) and placed in a quartz cuvette. A frequency-doubled laser system, 460 nm with a 76 MHz repetition rate, generated by a Ti:sapphire laser (Mira 900; Coherent, USA), was used as the excitation source. Fluorescence emission was detected by an R3809U multichannel plate photomultiplier tube (Hamamatsu Photonics K, Japan) and recorded by a fast counting card (EG&G Ortec 141, USA) to construct the fluorescence lifetime decay curve. In anisotropy relaxation experiments, the fluorescence emission with polarization parallel and perpendicular to the polarized excitation beam was measured and the anisotropy decay curves obtained by calculating the anisotropy from the parallel and perpendicular polarization decay curves (Lakowicz 1999). The rotational correlation time was obtained by fitting to a single/double exponential function (Lipari and Szabo 1980; Nettels et al. 2008).

**Fig. 2** spFRET results of AF488-m[C]q/S65C-AF594 trapped in the agarose gel. **a** Immobilized AF488-m[C]q/S65C-AF594 molecules (bright spots in the image) under confocal microscopy. The fluorescence emission intensity of the donor and acceptor for each single ubiquitin molecule was recorded over time. The corresponding FRET efficiency was calculated as a function of time according to the trajectories of the donor and acceptor fluorescence intensities and summarized in the FRET efficiency histogram. **b** and **c** Time trajectory of the donor (black) and acceptor (red) emission intensity and the corresponding FRET efficiency (upper panel in each) and the sub-FRET histogram (lower panel in each) for AF488-m[C]q/S65C-AF594 with high (**b**) and low (**c**) FRET efficiency. **d** Time trajectory of the molecule showing the transition from the high FRET state to the low FRET state

#### FRET data analysis

The FRET efficiency,  $E_{\text{ET}}$ , was calculated from the equation

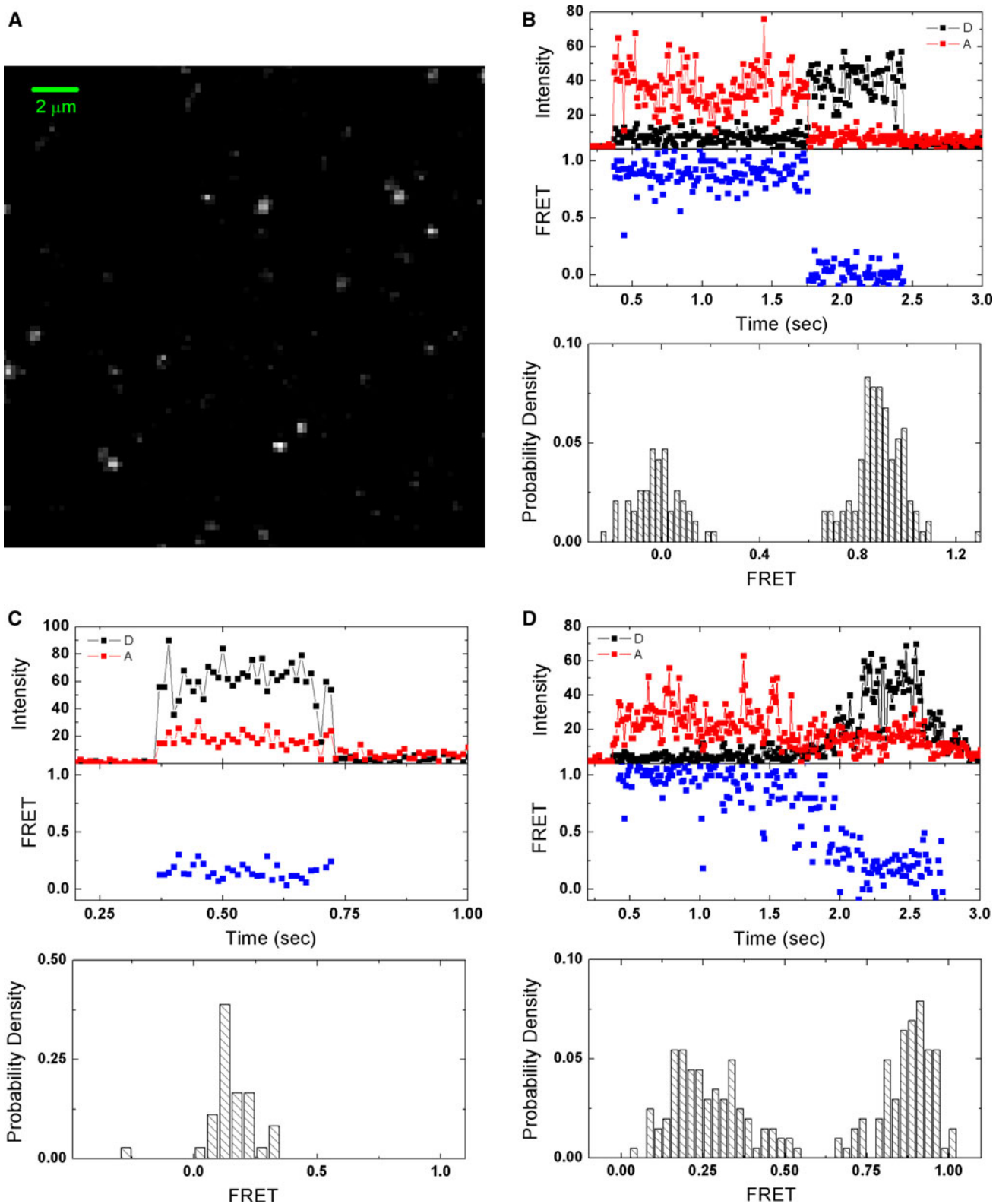
$$E_{\text{ET}} \equiv \frac{I_A}{I_A + I_D} = \frac{I_A^{\text{exp}} - \gamma \cdot \alpha \cdot I_D^{\text{exp}}}{I_A^{\text{exp}} + (1 - \gamma \cdot \alpha) \cdot I_D^{\text{exp}}},$$

where  $I_D^{\text{exp}}$  and  $I_A^{\text{exp}}$  are, respectively, the donor and acceptor emission intensity after subtracting their individual background value and  $\gamma$  is the correction factor for the difference in detection efficiency of the two detectors and quantum yields of dyes. The  $\gamma$  value was mainly governed by the difference in quantum efficiency between the two detectors, since the quantum yields of the donor and acceptor were equivalent according to our comparison of the fluorescence intensities of the free donor and acceptor. The  $\gamma$  value was measured from the emission intensity of thick-film poly[2-methoxy-5-(2'-ethyl-hexyloxy)-1,4-phenylenevinylene] (MEHPPV) in the donor and acceptor channels, the value obtained being 0.879.  $\alpha$  is the spectral leakage ratio from the donor to the acceptor channel and was measured as the acceptor/donor intensity ratio for the donor-only sample, AF488-m[C]q/S65C, the value obtained being 0.0245. Each spot was recorded for 10 s. The bin time was 10 ms. The thresholds for the donor and acceptor were adjusted manually. Several sets were tested to make sure the resulting histograms were unchanged. Molecules which had intensity above threshold (20 counts for either donor or acceptor channel) were selected. The intensity trajectories of the donor and acceptor were converted into a FRET trajectory.

## Results

### spFRET observation of AF488-m[C]q/S65C-AF594

To keep the labeled molecules at the focused laser spot long enough to investigate their conformational dynamics,



the protein was trapped in 1% agarose gel with pore size of about 600 nm, 200 times larger than the protein diameter (Narayanan et al. 2006; Pernodet et al. 1997), and the

protein-containing agarose gel film was sandwiched between two pure agarose gel films to maintain humidity during long-term observations (Fig. 1b) (Lu et al. 1998;

Yang et al. 2003). Based on our sample concentration (500 pM), the probability of two protein molecules being situated in the excitation focal volume was low ( $\sim 2.4\%$ ) (Chung et al. 2009). A homemade scanning-stage confocal microscope was used to locate the trapped protein molecules and to record the time traces of the donor and acceptor fluorescence intensities (Fig. 2a). Donor and acceptor photons were collected separately for each single molecule, and the data binned in 10 ms intervals. The FRET efficiency for each time point was calculated using the equation shown in the “Materials and methods” section. In the upper panel of Fig. 2b, the intensity–time trajectories of this molecule show high FRET efficiency. The conformational population of this molecule was calculated according to its survival time ( $\sim 2.2$  s for the molecule shown in Fig. 2b) in the FRET–time trajectories before both dyes were photobleached to construct its sub-FRET histogram (lower panel in Fig. 2b). In this sub-FRET histogram, it is obvious that the distributions have one peak centered at  $E_{ET} \approx 0.9$ , which is assumed to be the folded state, and another centered at around zero, which is attributed to acceptor photobleaching. Apart from the folded state, due to the decrease of protein stability of AF488-m[C]q/S65C-AF594, unfolded state was also detected. One unfolded molecule is shown in Fig. 2c. This molecule exhibited low FRET efficiency and had a peak at  $E_{ET} \approx 0.2$  in its sub-FRET histogram. Surprisingly, we can even find several molecules showing the structural transition from folded to unfolded state, as shown in Fig. 2d.

The trajectory of the fluorescent intensity versus time of a single fluorophore should show a typical one-step photobleaching behavior, while two molecules localized in the focal volume would show a two-step photobleaching behavior. Thus, when constructing the total FRET histogram, we excluded intensity–time trajectories not showing distinct one-step photobleaching behavior for both the donor and acceptor channel. A total of 221 molecules were used to build up the overall FRET histogram. The area of each sub-FRET histogram was fixed as 1, and the overall FRET histogram was constructed by summing the sub-FRET histograms of these molecules (Fig. 3a) (Hanson et al. 2007). The overall FRET histogram can be decomposed into four populations by fitting to four Gaussian distributions. The zero peak centered at  $E_{ET} = 0.03$  is due to a nonfunctional acceptor or an acceptor in the dark state. The peaks centered at  $E_{ET} = 0.22$  and  $E_{ET} = 0.95$  represent the unfolded and folded molecule, respectively. Beyond our expectation, a broad peak centered at  $E_{ET} = 0.72$  appeared in the overall FRET histogram. This peak was contributed by molecules showing moderate FRET efficiency, such as the molecule shown in Fig. 3b. This kind of molecules had FRET efficiency slightly lower

than the folded state. During the dye-labeling process it was noticed that the dye-labeled ubiquitin had much lower solubility, suggesting that some buried hydrophobic surface might be exposed after dye labeling. We surmised that the molecules showing moderate FRET efficiency might come from the loosely packed structure. The dynamic transition between the well-folded and the loosely packed structure were also recorded and are shown in Fig. 3c.

#### Compactness of the labeled protein

If dye labeling indeed affected protein packing, the loosely packed structure should be more susceptible to protease digestion. The compactness of dye-labeled ubiquitin and wild-type ubiquitin was examined by their resistance to trypsin digestion. As shown in Fig. 4, the donor-only labeled protein, AF488-m[C]q/S65C, was more sensitive to trypsin digestion, while the wild type was stable and protease resistant, suggesting that the structure of ubiquitin after dye labeling is less compact than that of wild-type ubiquitin.

#### Orientation dynamics of the dye

Time-resolved fluorescence depolarization was used to examine the rotational motions of the protein labeled with one dye molecule. Decaying anisotropy components with distinct relaxation times were assigned to different modes of motion, the rotational diffusion of the whole molecule (the dye-labeled protein), and the restricted dye rotation near the protein surface (Alexiev et al. 2003; Schuler et al. 2005). The side-chain of Ser65 in the crystal structure of ubiquitin is less solvent accessible than the side-chain of the cysteine in m[C]q. To confirm that the dye could still rotate freely after being linked to the side-chain of Ser65, we compared the anisotropy relaxation of pure donor dye (Alexa Fluor 488) and the donor-labeled S65C mutant protein (AF488-S65C) in solution. Alexa Fluor 488 was used here rather than Alexa Fluor 594 because of the available wavelength of our laser.

Relaxation of anisotropy is sensitive to rotational diffusion and shows exponential decay. For a protein with molecular mass of 10 kD, the rotational correlation time is around 3–5 ns at room temperature (Lakowicz 1999). As shown in Fig. 5, the anisotropy decay curve for AF488-S65C in solution showed a slower relaxation process (3.6 ns) and an initial fast phase ( $\sim 0.4$  ns), whereas the anisotropy relaxation of Alexa Fluor 488 was fitted by a single exponential decay ( $\sim 0.3$  ns). The fast correlation time ( $\sim 0.4$  ns) was therefore assigned to the combined motions of tumbling dye and the protein molecules, whereas the slower phase was directly attributed to rotation

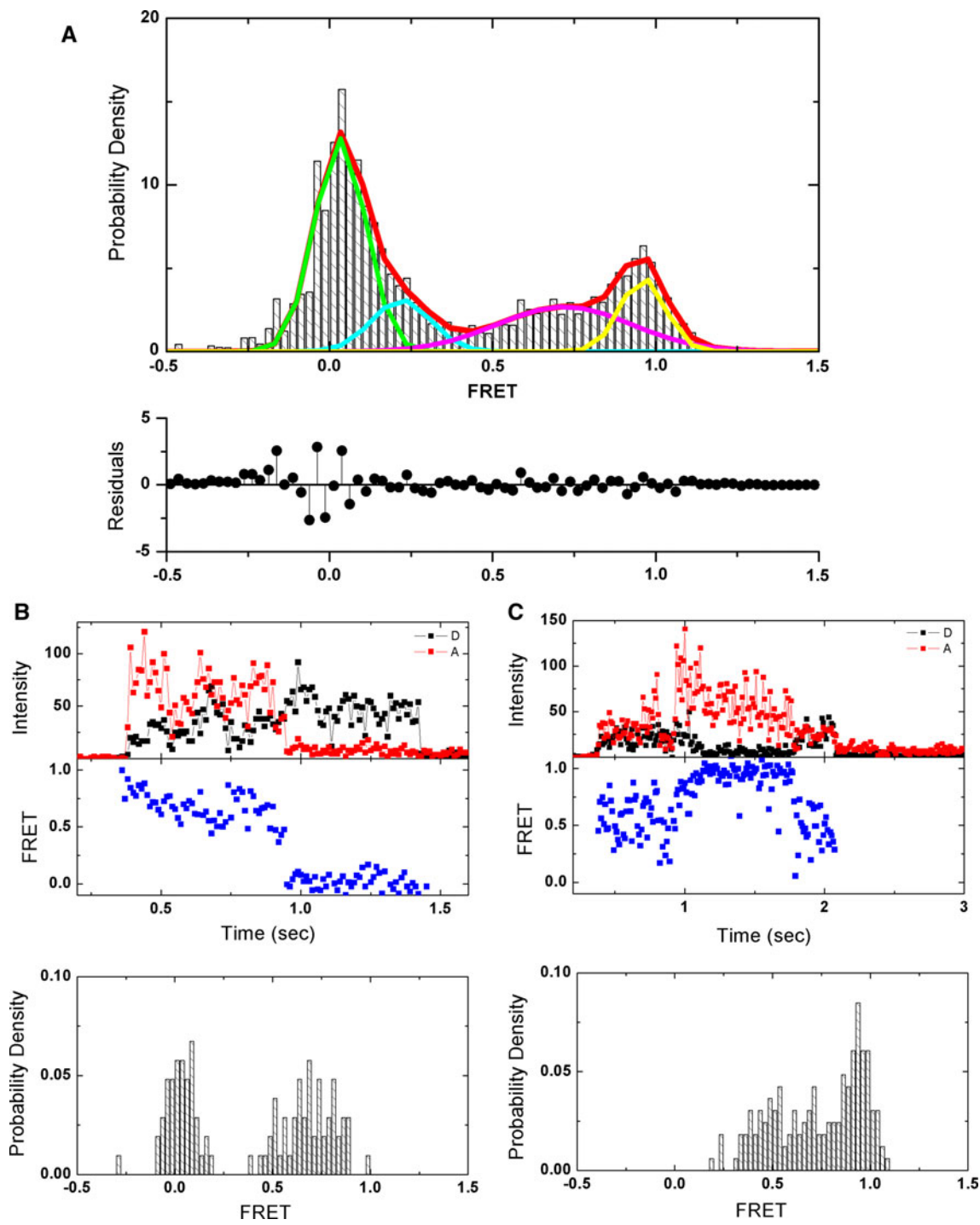


**Fig. 3** **a** Overall FRET histogram for 221 recorded molecules and the fitted results. The simulated curve is shown in red. The corresponding residuals are shown in the *lower panel*. **b** Time trajectory of the donor and acceptor emission intensity and the corresponding FRET efficiency (*upper panel* in each) and the sub-FRET histogram (*lower*

*panel* in each) for AF488-m[C]q/S65C-AF594 with moderate FRET efficiency. **c** Time trajectory of the molecule showing the transition from the moderate FRET state to the high FRET state and back to the moderate FRET state

of the dye-labeled protein (Alexiev et al. 2003; Lipari and Szabo 1980; Nettels et al. 2008). This indicates that the dye molecule bound to the protein was able to freely rotate, rather than being confined to a certain angle.

## Discussion

For single-molecule study, agarose gel has only been used in a few reports: Xie and coworkers studied the

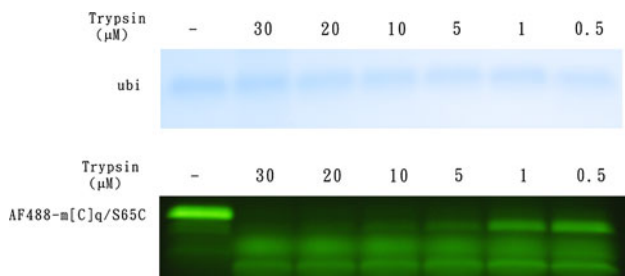


**Fig. 4** Comparison of the structural compactness of wild-type ubiquitin and dye-labeled ubiquitin (AF488-m[C]q/S65C) using trypsin digestion. Different concentrations of trypsin were used to digest the proteins at 37°C for 1 h

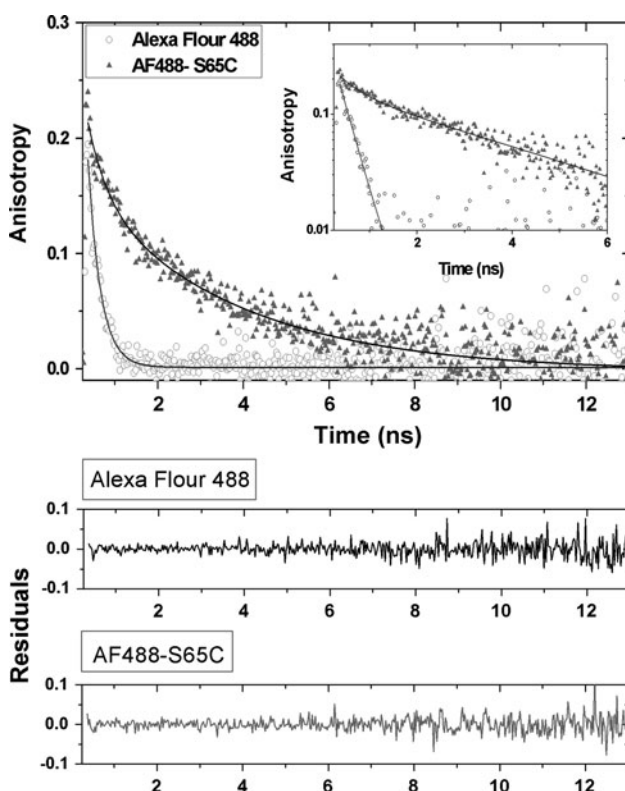


**Fig. 5** Time-resolved fluorescence anisotropy of Alexa Fluor 488 (open circles) and AF488-S65C (close triangles). The corresponding residuals are shown in the lower panels. (Inset time-resolved fluorescence anisotropy of Alexa Fluor 488 and AF488-S65C on semilog scale)

photochemistry of agarose-trapped allophycocyanin (Ying and Xie 1998) and the turnover of agarose-trapped cholesterol oxidase by monitoring the emission from the fluorescent flavin adenine dinucleotide (FAD) of the enzyme (Lu et al. 1998); Shi et al. (2006) studied the turnover of a flavoenzyme dihydroorotate dehydrogenase A; Segers-Nolten et al. (2002) used agarose as the immobilization method to monitor the bimolecular interaction between enhanced green fluorescent protein (EGFP)–xeroderma pigmentosum group A (XPA) protein

and Cy<sup>3,5</sup>-labeled DNA; and Allen et al. (2004) immobilized doubly labeled calmodulin–maltose binding protein (MBP) fusion protein in agarose to measure its binding with calmodulin-binding domain peptide. Our study showed that trapping in agarose gel is useful for monitoring the dynamic behavior of proteins in native condition. Three conformational populations with different FRET efficiencies were found for AF488-m[C]q/S65C-AF594. In addition, 46 in 221 molecules showed a transition between these conformational states. One population had low FRET efficiency ( $E_{ET}$  centered at 0.22), whereas the other two had higher FRET efficiencies ( $E_{ET}$  centered at 0.72 and 0.95). Based on the X-ray structure of ubiquitin (Vijay-Kumar et al. 1987), the distance between the donor and acceptor was estimated to be ~38 Å in the native state, and the corresponding FRET efficiency was calculated as about 0.94 on the basis of a Förster radius ( $R_0$ ) (Alexa Fluor 488 and Alexa Fluor 594) of ~60 Å (Molecular Probes). Thus, the high FRET state ( $E_{ET} = 0.95$ ) is very likely to be a conformer similar to that seen in the X-ray crystal study.

In addition to the anticipated native-like conformer with high FRET efficiency, a low FRET state ( $E_{ET} \approx 0.22$ ) and a moderate FRET state ( $E_{ET} \approx 0.72$ ) were also observed. We believe that the observed heterogeneity might be related to the decreased structural stability of the protein after dye labeling, as reported in our earlier study. We suggest that the population with the lowest FRET efficiency ( $E_{ET} \approx 0.22$ ) represents unfolded ubiquitin and that the switch from the highest FRET state ( $E_{ET} \approx 0.95$ ) to the lowest FRET state ( $E_{ET} \approx 0.22$ ), shown in Fig. 2d, represents the unfolding process. Dye labeling lowered the energy barrier between the folded and unfolded state and shifted the equilibrium toward the population in the unfolded state, making it possible to observe the presence of unfolded ubiquitin, even in water.

Regarding the population with moderate FRET efficiency ( $E_{ET} \approx 0.72$ ), we believe that this might be a “loosely packed form.” The trypsin digestion results clearly showed that AF488-m[C]q/S65C was more susceptible to protease digestion than wild-type ubiquitin (Fig. 4), suggesting that the structure of AF488-m[C]q/S65C is less compact. Compared with the folded population ( $E_{ET} \approx 0.95$ ), the population with  $E_{ET} \approx 0.72$  corresponded to an increase in the distance between the donor and acceptor from 38 to 51 Å. Recently, the issue of the nature of the dye molecule and its interplay with the labeled target in FRET studies has received attention (Chung et al. 2009, 2010). The fluorescence dyes used in our work contain a multiple-ring-conjugated structure with anionic solubilizing groups, which might interact with the protein and affect protein packing.

However, other possibilities other than the conformational dynamics discussed above should be considered. The

first is the flipping of the dipole orientation, which results from the rotation-constrained dye molecules. To clarify the issue of dipole orientations, we performed anisotropy depolarization measurements on both AF488-S65C and free Alexa Fluor 488, and the results (Fig. 5) showed that both free Alexa Fluor 488 and AF488-S65C shared a burst phase ( $\tau < 1$  ns) in the anisotropy relaxation curves, indicating that the dye on ubiquitin is freely rotating. Secondly, since our ubiquitin molecules were trapped in an agarose gel, the interaction between agarose and protein should be taken into account. Since 1% agarose gel consists of 99% water and the pores are 200 times larger than the protein size, the ubiquitin molecules were in an aqueous environment and protein movement was seen after a few days under a wide-field fluorescence microscope coupled to an electron-multiplying charge-coupled device (data not shown), suggesting that our protein was not bound to agarose. The third possibility is an artifact due to the nature of Alexa Fluor 488 (Chung et al. 2009), which was recently found to have another fluorescent state, denoted Alexa Fluor 488<sup>R</sup>, which had a emission spectrum red-shifted by  $\sim 25$  nm (Chung et al. 2009). This would lead to a longer Förster radius ( $R_0 \approx 62.5$  Å), and the same distance (38 Å) between the donor and acceptor estimated for native ubiquitin would thus correspond to a higher FRET efficiency ( $E_{ET} \approx 0.94 \rightarrow E_{ET} \approx 0.96$ ). However, the difference is very small and might just broaden the peaks rather than introducing a new population.

To sum up, agarose gel immobilization is a feasible method to observe dynamic behavior of single molecules. Because agarose cannot properly coagulate in the presence of denaturants such as urea or guanidine hydrochloride, this immobilizing method can only be applied in native condition. It could be applied to observe dynamic behavior of a protein during protein–protein or protein–ligand interactions.

**Acknowledgments** This work was supported by an Academia Sinica program project (AS-99-TP-AB5) and by the National Science Council, Taiwan, ROC (grant no. NSC 97-2113-M-001-014-MY2).

## References

Alexiev U, Rimke I, Pöhlmann T (2003) Elucidation of the nature of the conformational changes of the EF-interhelical loop in Bacteriorhodopsin and of the helix VIII on the cytoplasmic surface of Bovine Rhodopsin: a time-resolved fluorescence depolarization study. *J Mol Biol* 328:705–719

Allen MW, Urbauer RJ, Zaidi A, Williams TD, Urbauer JL, Johnson CK (2004) Fluorescence labeling, purification, and immobilization of a double cysteine mutant calmodulin fusion protein for single-molecule experiments. *Anal Biochem* 325:273–284

Benjamin S (2005) Single-molecule fluorescence spectroscopy of protein folding. *Chem Phys Chem* 6:1206–1220

Best RB, Merchant KA, Gopich IV, Schuler B, Bax A, Eaton WA (2007) Effect of flexibility and cis residues in single-molecule FRET studies of polyproline. *Proc Natl Acad Sci USA* 104:18964–18969

Chung HS, Louis JM, Eaton WA (2009) Experimental determination of upper bound for transition path times in protein folding from single-molecule photon-by-photon trajectories. *Proc Natl Acad Sci USA* 106:11837–11844

Chung HS, Louis JM, Eaton WA (2010) Distinguishing between protein dynamics and dye photophysics in single-molecule FRET experiments. *Biophys J* 98:696–706

Deniz AA, Laurence TA, Beligere GS, Dahan M, Martin AB, Chemla DS, Dawson PE, Schultz PG, Weiss S (2000) Single-molecule protein folding: diffusion fluorescence resonance energy transfer studies of the denaturation of chymotrypsin inhibitor 2. *Proc Natl Acad Sci USA* 97:5179–5184

Ha T, Ting AY, Liang J, Caldwell WB, Deniz AA, Chemla DS, Schultz PG, Weiss S (1999a) Single-molecule fluorescence spectroscopy of enzyme conformational dynamics and cleavage mechanism. *Proc Natl Acad Sci USA* 96:893–898

Ha T, Ting AY, Liang J, Deniz AA, Chemla DS, Schultz PG, Weiss S (1999b) Temporal fluctuations of fluorescence resonance energy transfer between two dyes conjugated to a single protein. *Chem Phys* 247:107–118

Hanson JA, Duderstadt K, Watkins LP, Bhattacharyya S, Brokaw J, Chu J-W, Yang H (2007) Illuminating the mechanistic roles of enzyme conformational dynamics. *Proc Natl Acad Sci USA* 104:18055–18060

Jacob MH, Amir D, Ratner V, Gussakowsky E, Haas E (2005) Predicting reactivities of protein surface cysteines as part of a strategy for selective multiple labeling. *Biochemistry* 44:13664–13672

Kao MW, Yang LL, Lin JC, Lim TS, Fann W, Chen RP (2008) Strategy for efficient site-specific FRET-dye labeling of ubiquitin. *Bioconjug Chem* 19:1124–1126

Kapanidis AN, Weiss S (2002) Fluorescent probes and bioconjugation chemistries for single-molecule fluorescence analysis of biomolecules. *J Chem Phys* 117:10953–10964

Kim Y, Ho SO, Gassman NR, Korlann Y, Landorf EV, Collart FR, Weiss S (2008) Efficient site-specific labeling of proteins via cysteines. *Bioconjug Chem* 19:786–791

Kuzmenkina EV, Heyes CD, Nienhaus GU (2005) Single-molecule Förster resonance energy transfer study of protein dynamics under denaturing conditions. *Proc Natl Acad Sci USA* 102:15471–15476

Kuzmenkina EV, Heyes CD, Nienhaus GU (2006) Single-molecule FRET study of denaturant induced unfolding of RNase H. *J Mol Biol* 357:313–324

Lakowicz JR (1999) Principles of fluorescence spectroscopy, 2nd edn. Springer, New York

Laurence TA, Kong X, Jager M, Weiss S (2005) Probing structural heterogeneities and fluctuations of nucleic acids and denatured proteins. *Proc Natl Acad Sci USA* 102:17348–17353

Lenkinski RE, Chen DM, Glickson JD, Goldstein G (1977) Nuclear magnetic resonance studies of the denaturation of ubiquitin. *Biochim Biophys Acta* 494:126–130

Lipari G, Szabo A (1980) Effect of librational motion on fluorescence depolarization and nuclear magnetic resonance relaxation in macromolecules and membranes. *Biophys J* 30:489–506

Lipman EA, Schuler B, Bakajin O, Eaton WA (2003) Single-molecule measurement of protein folding kinetics. *Science* 301:1233–1235

Lu HP, Xun L, Xie XS (1998) Single-molecule enzymatic dynamics. *Science* 282:1877–1882

Margittai M, Widengren J, Schweinberger E, Schroder GF, Felekyan S, Haustein E, Konig M, Fasshauer D, Grubmuller H, Jahn R, Seidel CAM (2003) Single-molecule fluorescence resonance energy transfer reveals a dynamic equilibrium between closed

and open conformations of syntaxin 1. *Proc Natl Acad Sci USA* 100:15516–15521

Merchant KA, Best RB, Louis JM, Gopich IV, Eaton WA (2007) Characterizing the unfolded states of proteins using single-molecule FRET spectroscopy and molecular simulations. *Proc Natl Acad Sci USA* 104:1528–1533

Narayanan J, Xiong J-Y, Liu X-Y (2006) Determination of agarose gel pore size: absorbance measurements vis a vis other techniques. *J Biophys Conf Ser* 28:83–86

Nettels D, Hoffmann A, Schuler B (2008) Unfolded protein and peptide dynamics investigated with single-molecule FRET and correlation spectroscopy from picoseconds to seconds. *J Phys Chem B* 112:6137–6146

Orte A, Craggs TD, White SS, Jackson SE, Klenerman D (2008) Evidence of an intermediate and parallel pathways in protein unfolding from single-molecule fluorescence. *J Am Chem Soc* 130:7898–7907

Pernodet N, Maaloum M, Tinland B (1997) Pore size of agarose gels by atomic force microscopy. *Electrophoresis* 18:55–58

Ratner V, Sinev M, Haas E (2000) Determination of intramolecular distance distribution during protein folding on the millisecond timescale. *J Mol Biol* 299:1363–1371

Rhoades E, Gussakovskiy E, Haran G (2003) Watching proteins fold one molecule at a time. *Proc Natl Acad Sci USA* 100:3197–3202

Rhoades E, Cohen M, Schuler B, Haran G (2004) Two-state folding observed in individual protein molecules. *J Am Chem Soc* 126:14686–14687

Schuler B, Lipman EA, Eaton WA (2002) Probing the free-energy surface for protein folding with single-molecule fluorescence spectroscopy. *Nature* 419:743–747

Schuler B, Lipman EA, Steinbach PJ, Kumke M, Eaton WA (2005) Proline and the “spectroscopic ruler” revisited with single-molecule fluorescence. *Proc Natl Acad Sci USA* 102:2754–2759

Segers-Nolten GMJ, Wyman C, Wijgers N, Vermeulen W, Lenferink ATM, Hoeijmakers JHJ, Greve J, Otto C (2002) Scanning confocal fluorescence microscopy for single molecule analysis of nucleotide excision repair complexes. *Nucleic Acids Res* 30:4720–4727

Shi J, Dertouzos J, Gafni A, Steel D, Palfey BA (2006) Single-molecule kinetics reveals signatures of half-sites reactivity in dihydroorotate dehydrogenase a catalysis. *Proc Natl Acad Sci USA* 103:5775–5780

Tan Y-W, Hanson JA, Yang H (2009) Direct Mg<sup>2+</sup> binding activates adenylate kinase from *Escherichia coli*. *J Biol Chem* 284:3306–3313

Vijay-Kumar S, Bugg CE, Cook WJ (1987) Structure of ubiquitin refined at 1.8 Å resolution. *J Mol Biol* 194:531–544

Weiss S (2000) Measuring conformational dynamics of biomolecules by single molecule fluorescence spectroscopy. *Nat Struct Biol* 7:724–729

Yang H, Luo G, Karnchanaphanurach P, Louie T-M, Rech I, Cova S, Xun L, Xie XS (2003) Protein conformational dynamics probed by single-molecule electron transfer. *Science* 302:262–266

Ying L, Xie XS (1998) Fluorescence spectroscopy, exciton dynamics, and photochemistry of single allophycocyanin trimers. *J Phys Chem B* 102:10399–10409